



Electrospun poly(lactic acid)/chitosan core-shell structure nanofibers from homogeneous solution

Yajing Li, Fan Chen, Jun Nie, Dongzhi Yang*

State Key Laboratory of Chemical Resource Engineering, Key Laboratory of Beijing City on Preparation and Processing of Novel Polymer Materials, Beijing University of Chemical Technology, Beijing 100029, China

ARTICLE INFO

Article history:

Received 17 April 2012

Received in revised form 2 July 2012

Accepted 3 July 2012

Available online 13 July 2012

Keywords:

Core-shell structure

Electrospinning

Poly(lactic acid)

Homogeneous solution

Chitosan

ABSTRACT

The core-shell structure nanofibers of poly(lactic acid)/chitosan with different weight ratios were successfully electrospun from homogeneous solution. The preparation process was more simple and effective than double-needle electrospinning. The nanofibers were obtained with chitosan in shell while poly(lactic acid) in core attributing to phase separation, which were characterized by scanning electron microscopy (SEM), transmission electron microscopy (TEM), X-ray diffraction (XRD) and energy dispersive spectrometer (EDS). The electrospun nanofibrous membrane was evaluated in vitro by using mouse fibroblasts (L929) as reference cell lines. Cell culture results indicated that these materials were good in promoting cell growth and attachment, thus they could be used for tissue engineering and wound healing dressing.

© 2012 Elsevier Ltd. All rights reserved.

1. Introduction

Electrospinning is currently one of the most versatile and effective methods used in the manufacturing of nanoscale fibers. The nanofibrous membranes prepared by electrospinning have several advantages such as, extremely large specific surface area, high porosity. However, what makes electrospinning different from other nanofiber fabrication processes is its ability to form various sizes of fibers or substance assemblies. As well as, the mild operating conditions of electrospinning are beneficial for loading many biologically active substances (Bhardwaj & Kundu, 2010; Chronakis, 2005; Liang, Hsiao, & Chu, 2007).

Because of the excellent biological properties, such as biodegradability, nontoxicity, antibacterial ability and biocompatibility, chitosan (CS) composite electrospun membrane has been known as promising material in many biomedical fields from skin to bone or cartilage (Alves & Mano, 2008; MacNei, 2007; Mano et al., 2007). However, the scaling-up of CS nanofiber fabrication by electrospinning is problematic and challenging. Due to its polyelectrolyte nature, CS cannot be continuously spun as droplets persistently form (Muzzarelli, 2011). Neat CS electrospun membrane has some other significant shortcomings as well: poor mechanical strength, especially in vitro, chitosan hydrolysis might happen under the conditions of water or tissue fluid. To solve

these problems, blending CS with some water-soluble polymers was available to make CS electrospinnable. In the previous report, poly(ethylene oxide) (PEO) and poly(vinyl alcohol) (PVA) were the most commonly employed to help the fabrication of chitosan-based nanofibers (Jia et al., 2007; Ojha et al., 2008; Shalumon et al., 2009; Zhang et al., 2008). Some studies in our group about CS blended with PVA or PEO electrospun nanofibrous membrane have been reported for the applications of tissue engineering scaffolds and wound healing dressings (Yang et al., 2008; Zhou et al., 2008).

The hydrophobic polyester poly(lactic acid) (PLA) has good mechanical property and biocompatibility. The preparation of blending electrospun PLA and CS nanofibrous membrane from homogeneous solution might overcome some drawbacks of CS alone (Sun & Li, 2011). Some works have been devoted to manufacturing PLA/CS composites. Peesan, Rujiravanit, and Supaphol (2006) had prepared PLA/hexanoyl chitosan blend electrospinning fibers by using chloroform, dichloromethane (DCM) or tetrahydrofuran (THF) as solvent, respectively. Ignatova, Manolova, Markova, and Rashkov (2009) prepared PLA/CS electrospinning nanofibrous mats with the mixed solution of chitosan or its quaternized derivative and PLA in trifluoroacetic acid (TFA) or dimethylformamide (DMF). Electrospun nanofibrous mats containing quaternized chitosan and PLA against HeLa cells were also investigated (Ignatova et al., 2010). Nguyen, Chung, and Park (2011) fabricated PLA/CS non-woven mats using coaxial electrospinning process in trifluoroacetic acid (TFA). The PLA/CS core-shell composite nanofibers showed antibacterial activity against *Escherichia coli*. Huang et al. (2007) had described co-axial electrospinning

* Corresponding author. Tel.: +86 1064421310; fax: +86 1064421310.
E-mail address: yangdz@mail.buct.edu.cn (D. Yang).

process to fabricate double-layered ultrafine fibers. However, as we all know, due to the different types of solvent used in core and shell layers, poor continuity, low yield and instability of processing are the biggest obstacles in the popular application of core-shell electrospinning by double-needle.

In this study, we aim to develop one kind of PLA (core)/CS (shell) nanofibrous membrane by a facile way. The single nozzle electrospinning with homogeneous solution is more simple and effective than double-needle electrospinning for preparing continuous core-shell nanofibers. PLA was chosen as core material because of its excellent biocompatibility, mechanical property and good electrospinning fiber-forming ability. As mentioned above, neat CS was difficult to form continuous nanofibers by electrospinning because of its poor mechanical property. In order to form homogeneous solution, sodium dodecyl sulfate (SDS) was employed to modify CS. SDS which was on the surface of PLA/SDS-CS nanofibrous membrane could be easily removed. The nanofibers were obtained with CS in shell while PLA in core attributing to phase separation, which were characterized by SEM, TEM, XRD, EDS. L929 cell culture and adhesion on the surface of nanofibrous membrane were also evaluated. It suggested that the composite was an appropriate candidate for tissue engineering and wound dressing in biomedical filed.

2. Experimental

2.1. Materials

Chitosan ($\overline{M}_w = 3000$ g/mol, 8000 g/mol; degree of deacetylation = 88%) was purchased from Zhejiang Golden-Shell Biochemical Co. Ltd. (Yuhuan, Zhejiang, China). PLA (150 kDa) was supplied by Beijing Huabo Union Biodegradable Materials Technologies Co. Ltd. (Beijing, China). Sodium dodecyl sulfate (SDS) and other reagents were purchased from Beijing Chemical Reagent Company and used without further purification.

2.2. Preparation and characterization of chitosan derivative (SDS-CS)

Chitosan (1.6 g) was dissolved in 50 mL 2 wt% acetic acid solution. Excess SDS (8.2771 g) was dissolved in 50 mL distilled water. The above mixed solution was constantly stirred into homogeneous solution for 4 h at 25 °C. SDS-CS was precipitated from the mixed solution, then was collected by high-speed centrifugation and washed with deionized water. Finally, the white powder SDS-CS was obtained from freeze-drying.

FTIR spectra of CS, SDS-CS and electrospinning nanofibers were recorded by a Nicolet 5700 FTIR spectrometer (Nicolet Instrument, Thermo Company, Madison, USA). The samples were prepared as KBr pellets and scanned against a blank KBr pellet background at wavenumber range of 4000–700 cm^{-1} with resolution of 4.0 cm^{-1} .

2.3. Preparation of homogeneous solution and electrospinning

PLA and SDS-CS were dissolved in dichloromethane (DCM) and dimethyl sulfoxide (DMSO) respectively, then two kinds of transparent solution were mixed into homogeneous solution with different weight ratios. (PLA/SDS-CS = 80/20; 70/30; 60/40; 50/50; 40/60; 20/80. Neat PLA solution was marked as PLA/SDS-CS = 100/0 for comparison). The electrospinning PLA/SDS-CS solution was prepared with the total concentration of 3%.

The electrospinning was performed at room temperature. The above mixed solution was placed into a plastic syringe (5 mL) equipped with a single nozzle. The electrospinning conditions were set as follows: The solution was supplied by a syringe pump which

maintained at a constant feed rate of 0.01 mm/s. The positive electrode of a high voltage (20 kV) power supply (BG4-21, BMEI Co. Ltd., China) was applied between the syringe tip and collector. An aluminum foil was used as the collector, tip-to-collector distance was fixed at 20 cm. The nanofibrous membranes were collected on the surface of aluminum foil and dried at room temperature in vacuum for 24 h.

2.4. Cross-linking of the electrospun membranes

PLA/SDS-CS electrospun nanofibrous membranes were immersed in 15 wt% tris-base solution for 1 h to wash away SDS which was on the surface of membranes and then rinsed with deionized water for 3 h, changing water in every 30 min. The membranes then were washed with ethanol to remove the residual solvent. The PLA/CS nanofibrous membranes obtained above were further cross-linked in the glutaraldehyde vapor at room temperature for 2 days. After cross-linking, the membranes were immersed in deionized water to remove the untreated glutaraldehyde. The cross-linked membranes were dried at 60 °C in vacuum for 24 h and prepared for further cell culture and adhesion in vitro study.

2.5. Scanning electron microscopy (SEM)

The morphology of nanofibrous membranes sputter-coated with gold was observed by a scanning electron microscope (Hitachi S-4700, Hitachi Company, Japan) with an accelerating voltage of 20 kV. The average diameter of nanofibers was determined randomly by image analysis tool (Image-J, National institutes of Health U.S.) to analyze 100 different fibers from a SEM image.

2.6. Transmission electron microscopy (TEM) and energy dispersive spectrometer (EDS)

The core-shell structure of the nanofibers was characterized by transmission electron microscopy (TEM, JEM3010 JEOL) with an energy dispersive spectrometer (EDS). EDS was used in conjunction with TEM for elemental analysis of the shell layer component of the electrospun nanofibers.

2.7. X-ray diffraction (XRD)

The XRD patterns of the samples were recorded on a wide-angle X-ray diffraction analyzer (WAXD, D/Max 2500 VB2+/PC, Rigaku Company, Tokyo, Japan) under area detector operating at a voltage of 40 kV and a current of 50 mA using Cu K α radiation ($\lambda = 0.154$ nm). The scanning rate was 1°/min in the 2θ range from 5° to 60°.

2.8. Cell culture and adhesion

The cross-linked PLA/CS nanofibrous membranes were cut into 3 cm \times 3 cm samples (about 0.3 mm in thickness) and fixed on glass cover slips. After high-pressure steam sterilization for 20 min, the samples were transferred to individual 6-well tissue culture plates. The mouse fibroblast cells (L929) were cultured in DMEM medium supplemented with 10% fetal bovine serum, together with 1% penicillin streptomycin and 1.2% glutamine. Aliquots (1 mL) of L929 with 5×10^4 cell/mL were seeded on the sample membranes. Culture was maintained at 37 °C in a wet atmosphere containing 5% CO₂. After 48 h of culture, the samples were harvested and rinsed twice with PBS to remove non-adherent cells. After the staining of L929 for nuclei with 20 μL DAPI stock solution (1 mg/mL) for 5 min,

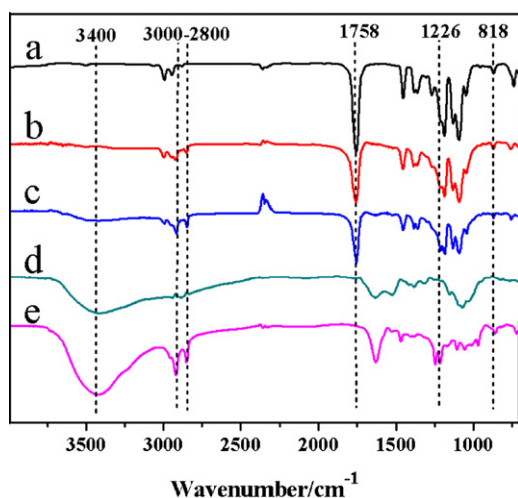


Fig. 1. FTIR spectra of electrospun pure PLA nanofibers (a); electrospun PLA/SDS-CS blend nanofibers with different weight ratios: PLA/SDS-CS = 80/20 (b); PLA/SDS-CS = 60/40 (c); pure CS (d); SDS modified CS (e).

the samples were observed by fluorescence microscope (Olympus BX41, Olympus Corporation, Japan) for cell adhesion.

3. Results and discussion

3.1. FTIR analysis

Fourier transform infrared spectroscopy (FTIR) data manifested very important information about the inter-molecular and intra-molecular interactions in polymers. Fig. 1 displayed the FTIR spectra of neat electrospun PLA fibers and PLA/SDS-CS blend fibers with different weight ratios, neat CS and SDS modified CS powder.

Compared with CS, the infra-red data of SDS modified CS showed the characteristic peaks at 1226 cm^{-1} (RO-SO₃⁻ stretch) and 818 cm^{-1} (S-O stretch). The absorption bands at $2800\text{--}3000\text{ cm}^{-1}$ (—CH₂ stretch) significantly increased due to the existence of SDS. The result suggested SDS has been coupled onto the amino group of CS. The broad band at around 3400 cm^{-1} could be obviously observed (—NH₂ and —OH stretches). The coupling effect of —NH₃⁺ and —SO₃⁻ broadened the shape of the peak, but the peak position did not change.

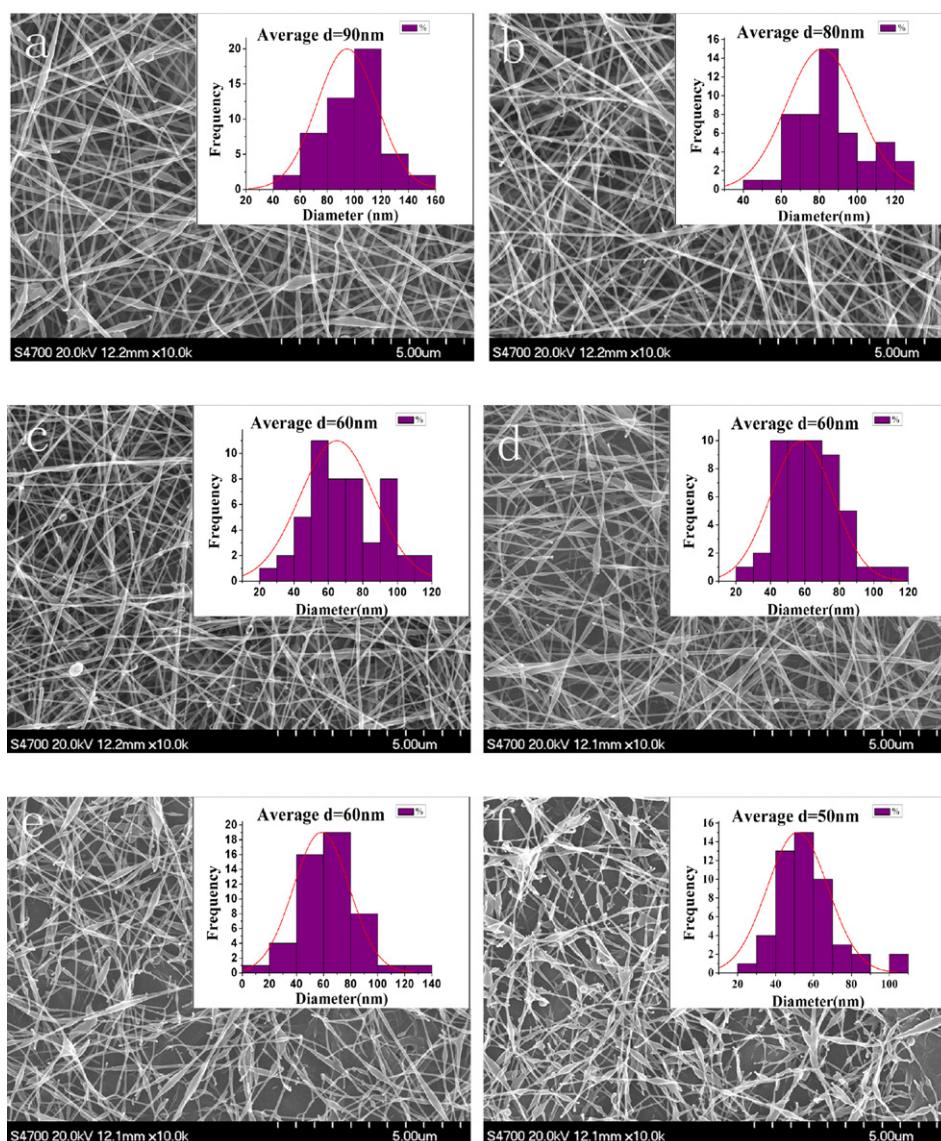


Fig. 2. SEM images and diameter distribution of electrospun PLA/SDS-CS nanofibers with different weight ratios: (a) PLA/SDS-CS = 100/0; (b) PLA/SDS-CS = 80/20; (c) PLA/SDS-CS = 70/30; (d) PLA/SDS-CS = 60/40; (e) PLA/SDS-CS = 50/50; (f) PLA/SDS-CS = 40/60.

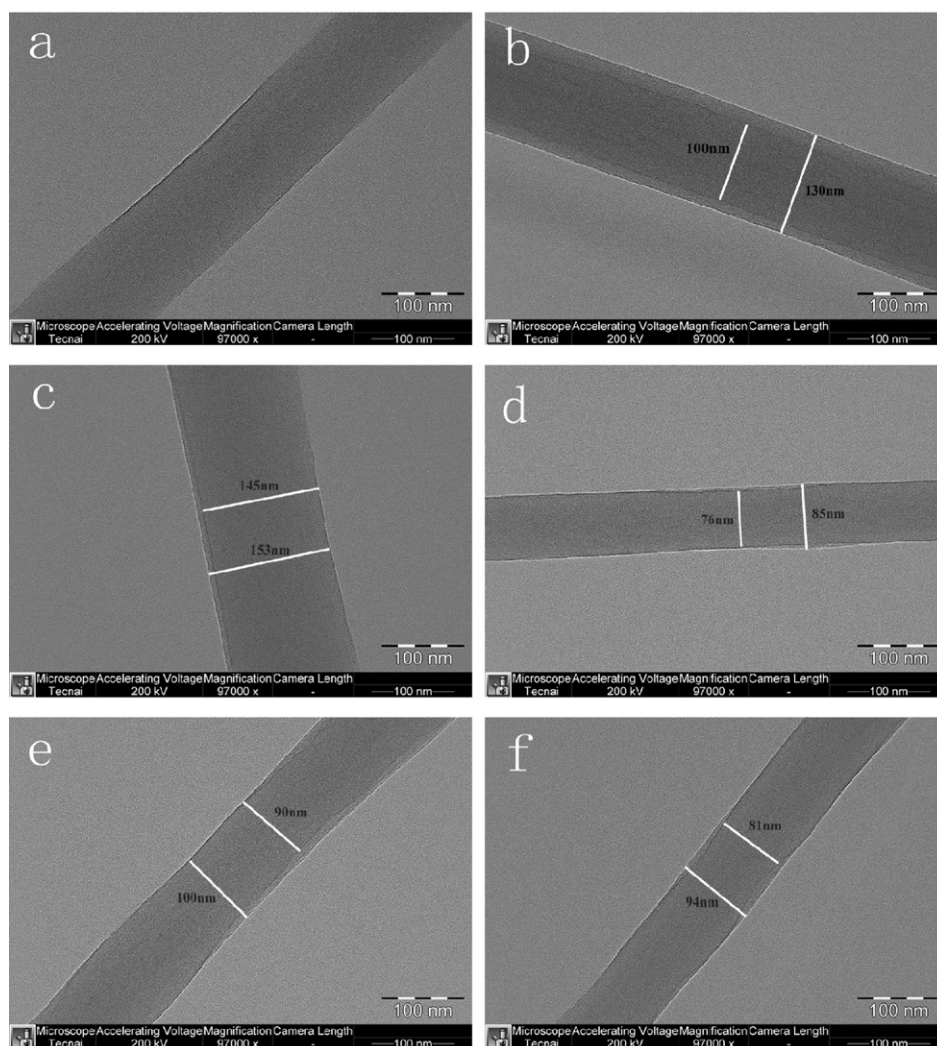


Fig. 3. TEM images of PLA/SDS-CS nanofibers with different weight ratios: (a) PLA/SDS-CS = 100/0; (b) PLA/SDS-CS = 80/20; (c) PLA/SDS-CS = 70/30; (d) PLA/SDS-CS = 60/40; (e) PLA/SDS-CS = 50/50; (f) PLA/SDS-CS = 40/60.

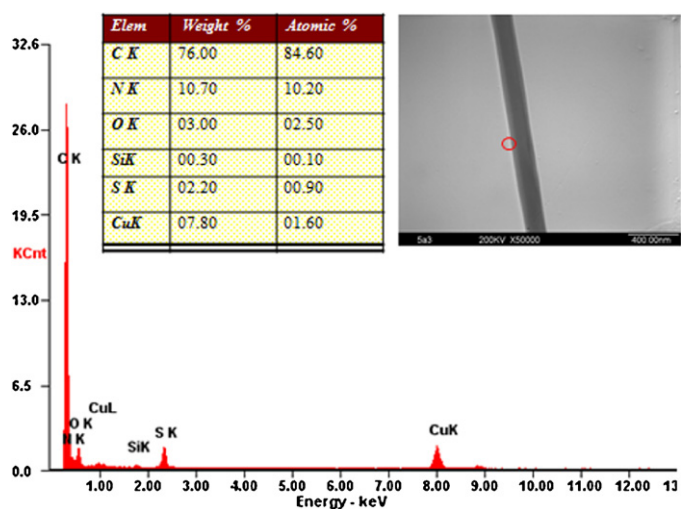


Fig. 4. TEM image and EDS analysis of PLA/SDS-CS ($\overline{M}_w = 3000$ g/mol) nanofibers, the inset circle within the confines of shell layer was for EDS analysis. (For interpretation of the references to color in text, the reader is referred to the web version of the article.)

The FTIR spectra of neat electrospun PLA and PLA/SDS-CS nanofibers (Fig. 1(a)–(c)) revealed characteristic absorption bands at 1758, 1187, 1131 and 1093 cm^{-1} , corresponding to the backbone ester group of PLA. With the increase of chitosan, the peak of 1758 cm^{-1} which belonged to the carbonyl group in PLA was decreased. It could be explained that the molecular interaction between PLA and SDS-CS was weak since the peaks position of these spectra almost did not change.

3.2. Surface morphology and distribution of PLA/SDS-CS nanofibers

The morphology of electrospun nanofibers and the fibers diameter were significantly influenced by the composition of electrospinning solution (Spasova, Manolova, Paneva, & Rashkov, 2006; Zhang, Yuan, Wu, Han, & Sheng, 2005). The SEM micrographs and diameter distributions of electrospun PLA/SDS-CS nanofibers with different weight ratios from 100/0 to 40/60 were shown in Fig. 2. With SDS-CS increasing, it was difficult to form continuous nanofibers, the nanofibers might show a large number of beaded structure. It could be seen that the uniform ultrafine electrospun PLA/SDS-CS nanofibers had smooth and homogeneous morphology (Fig. 2(a–c)). Neat PLA nanofibers had the highest average diameter (90 nm). With the increasing proportion of CS, the

average diameter of the nanofibers gradually decreased. Generally, it was known that CS was a polyelectrolyte and electrospinning of polymers with higher polarity provided nanofibers with smaller diameters. Additionally, the influence of CS with lower weight could be explained by strong mobility. In this case, the PLA/SDS-CS solution was stretched into thinner fibers with smaller diameters than neat PLA nanofibers.

3.3. Core-shell structure of PLA/SDS-CS nanofibers

Fig. 3 displayed TEM images of the core-shell structure of PLA/SDS-CS nanofibers with different weight ratios. The EDS analysis and TEM image were shown in Fig. 4. The inset red circle within the confines of shell layer in TEM image was for EDS analysis. The results indicated that the bright region was shell layer (SDS-CS) by detecting the major elements of nitrogen (N) and sulfur (S) on the surface of the nanofibers.

The formation of core-shell structure might be caused by the bimodal phase separation. The influence of CS molecular weight on diameter of core fiber might be explained by mobility and interaction of the polymer chain (Moghe & Gupta, 2008). For the lower molecular weight CS ($M_w = 3000$ g/mol), it had strong mobility. This was the reason why phase separation happened and resulting in small core fiber. With the content of CS increased, the core-shell structure was difficult to be observed.

Another reason for the accumulation of CS in the shell layer might attribute to the positive charged groups of CS generating in aqueous solution. During the electrospinning, the charged groups preferred to move out with the influence of electrical field (Zhang et al., 2009).

3.4. XRD spectra

Wide-angle X-ray diffraction was utilized to reveal the crystalline structure of electrospun nanofibers. Fig. 5 illustrated XRD patterns of PLA nanofibers, SDS-CS and PLA/SDS-CS nanofibers

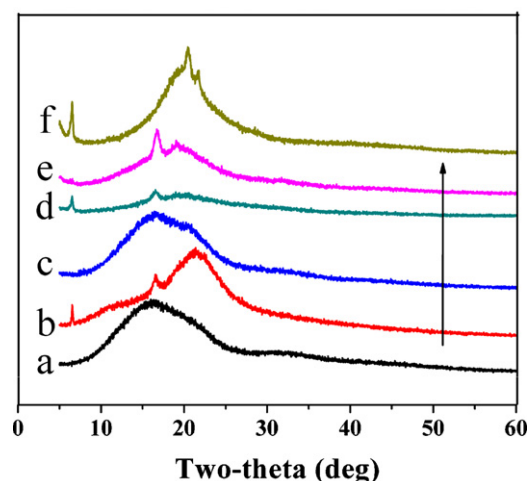


Fig. 5. XRD patterns of pure PLA nanofibers (a); PLA/SDS-CS ($M_w = 3000$ g/mol) = 80/20 (b); PLA/SDS-CS ($M_w = 8000$ g/mol) = 80/20 (c); PLA/SDS-CS ($M_w = 3000$ g/mol) = 60/40 (d); PLA/SDS-CS ($M_w = 8000$ g/mol) = 60/40 (e); SDS-CS powder (f).

with different weight ratios. SDS-CS was a semi-crystal polymer and its XRD patterns exhibited a sharp diffraction peaks at the scattering angle of 6.5° and 20.5° . The sharp diffraction peaks might be explained by SDS existing along the molecular chains to form crystal structure. Increasing number and improving arrangement of chains led to the increase of crystallinity. For neat PLA nanofibers, the obtained XRD pattern manifested only broad diffraction peak centering at 2θ of 17.5° . The obtained diffraction patterns of PLA/SDS-CS nanofibers with different weight ratios exhibited almost the same shape as SDS-CS powder, but the position of the peaks changed into the angle between 15° and 20° . This might be caused by the influence of amorphous structure with the existence of PLA.

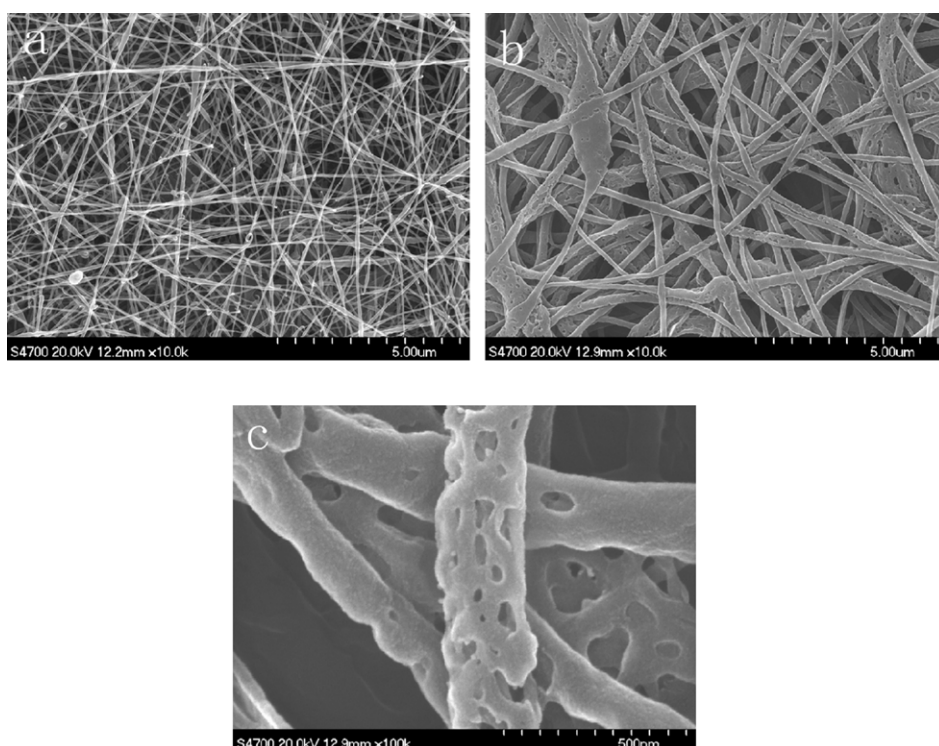


Fig. 6. SEM images on the surface of PLA/SDS-CS (70/30) nanofibers: (a) pretreatment, before SDS removed; (b) and (c) after SDS removed.

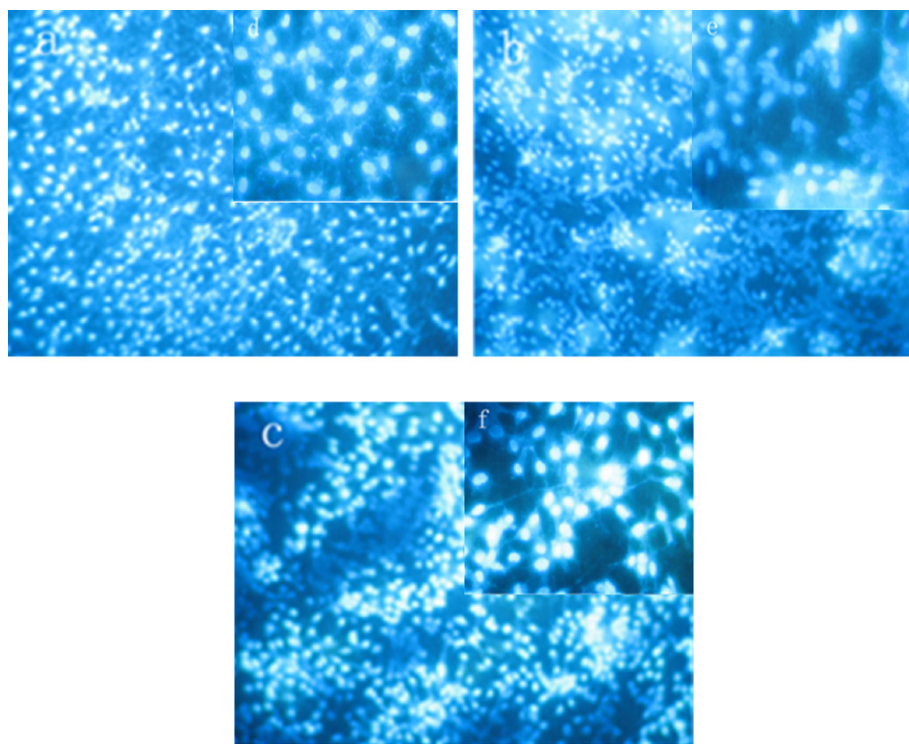


Fig. 7. Fluorescence micrographs of L929 fibroblasts on PLA/CS nanofibers with different weight ratios: (a) PLA/CS = 100/0, 100 \times ; (b) PLA/CS = 80/20, 100 \times ; (c) PLA/CS = 50/50, 100 \times ; (d) PLA/CS = 100/0, 400 \times ; (e) PLA/CS = 80/20, 400 \times ; (f) PLA/CS = 50/50, 400 \times .

3.5. Surface morphology of PLA/SDS-CS nanofibers before and after SDS removed

In this study, modification of CS with SDS did not form a strong covalent bond, but by electrostatic interaction. Therefore, the process of modification was reversible. Tris-base was chosen to treat PLA/SDS-CS nanofibers (70/30) to take off the SDS molecule, and then deionized water was used to remove SDS molecule which was on the surface of CS. SEM results after removing were shown in Fig. 6(b and c). It was obvious that there were plenty of washed erosion holes on the surface of nanofibers compared with the pre-treatment (Fig. 6(a)). It could be convinced that the shell layer of nanofibers composed of modified CS.

3.6. Adhesion and spreading of fibroblasts on PLA/CS nanofibers

To evaluate the cell growth and adhesion on PLA/CS nanofibers in vitro, L929 mouse fibroblasts cells were used. Fig. 7 showed fluorescence micrographs at two different magnifications (100 \times and 400 \times) of PLA/CS nanofibers with different weight ratios. As shown in Fig. 7, it could be seen that L929 cells exhibited a spreading tendency on PLA/CS nanofibers, the spindle shape and normal cell nucleus morphology suggested that the cells could function biologically on this material and PLA/CS nanofibrous membranes were available for cell adhesion.

4. Conclusions

A simple and effective method was demonstrated for the fabrication of core-shell structure of PLA/CS nanofibers with different weight ratios. SDS was employed to modify CS and FTIR analysis result proved the existence of SDS. Core-shell structure of nanofibers could be easily observed in TEM images. EDS analysis and SEM images of PLA/CS nanofibers before and after treated with water were induced to verify that CS was the major component

of the shell layer. L929 cell culture suggested that the nanofibrous membranes did well in promoting cell adhesion and proliferation. These materials had the potential to be used for tissue engineering and wound healing dressing.

Acknowledgments

The author would like to thank the National Natural Science Foundation of China (50803004), the Beijing Natural Science Foundation (2112033, Study on the molecular design and properties of new photocurable antifouling coatings) and the Fundamental Research Funds for the Central Universities (ZZ1115) for its financial support.

References

- Alves, N. M., & Mano, J. F. (2008). Chitosan derivatives obtained by chemical modifications for biomedical and environmental applications. *International Journal of Biological Macromolecules*, 43, 401–414.
- Bhardwaj, N., & Kundu, S. C. (2010). Electrospinning: A fascinating fiber fabrication technique. *Biotechnology Advances*, 28, 325–347.
- Chronakis, I. S. (2005). Novel nanocomposites and nanoceramics based on polymer nanofibers using electrospinning process: A review. *Journal of Materials Processing Technology*, 167, 283–293.
- Huang, Z. M., He, C. L., Yang, A. Z., Zhang, Y. Z., Han, X. J., Yin, J. L., et al. (2007). Encapsulating drugs in biodegradable ultrafine fibers through co-axial electrospinning. *Journal of Biomedical Materials Research Part A*, 77A, 169–179.
- Ignatova, M. G., Manolova, N. E., Markova, N., & Rashkov, I. (2009). Electrospun non-woven nanofibrous hybrid mats based on chitosan and PLA for wound dressing applications. *Macromolecular Bioscience*, 9, 102–111.
- Ignatova, M. G., Manolova, N. E., Toshkova, R. A., Rashkov, I. B., Gardeva, E. G., Yossifova, L. S., et al. (2010). Electrospun nanofibrous mats containing quaternized chitosan and polylactide with in vitro antitumor activity against HeLa cells. *Biomacromolecules*, 11, 1633–1645.
- Jia, Y. T., Gong, J., Gu, X. H., Kim, H. Y., Dong, J., & Shen, X. Y. (2007). Fabrication and characterization of poly(vinyl alcohol)/chitosan blend nanofibers produced by electrospinning method. *Carbohydrate Polymers*, 67, 403–409.
- Liang, D., Hsiao, B. S., & Chu, B. (2007). Functional electrospun nanofibrous scaffolds for biomedical applications. *Advanced Drug Delivery Reviews*, 59, 1392–1412.
- MacNeil, S. (2007). Progress and opportunities for tissue-engineered skin. *Nature*, 445, 874–880.

- Mano, J. F., Silva, G. A., Azevedo, H. S., Malafaya, P. B., Sousa, R. A., Silva, S. S., et al. (2007). Natural origin biodegradable systems in tissue engineering and regenerative medicine: Present status and some moving trends. *Journal of the Royal Society Interface*, 4, 999–1030.
- Moghe, A. K., & Gupta, B. S. (2008). Co-axial electrospinning for nanofiber structures: Preparation and applications. *Polymer Reviews*, 48, 353–377.
- Muzzarelli, R. A. A. (2011). Biomedical exploitation of chitin and chitosan via mechano-chemical disassembly, electrospinning, dissolution in imidazolium ionic liquids, and supercritical drying. *Marine Drugs*, 9, 1510–1533.
- Nguyen, T. T. T., Chung, O. H., & Park, J. S. (2011). Coaxial electrospun poly(lactic acid)/chitosan(core/shell) composite nanofibers and their antibacterial activity. *Carbohydrate Polymers*, 86, 1799–1806.
- Ojha, S. S., Stevens, D. R., Hoffman, T. J., Stano, K., Klossner, R., Scott, M. C., et al. (2008). Fabrication and characterization of electrospun chitosan nanofibers formed via templating with polyethylene oxide. *Biomacromolecules*, 9, 2523–2529.
- Peesan, M., Rujiravanit, R., & Supaphol, P. (2006). Electrospinning of hexanoyl chitosan/poly(lactide) blends. *Journal of Biomaterials Science, Polymer Edition*, 17, 547–565.
- Shalumon, K. T., Binulal, N. S., Selvamurugan, N., Nair, S. V., Menon, D., Furuike, T., et al. (2009). Electrospinning of carboxymethyl chitin/poly(vinyl alcohol) nanofibers scaffolds for tissue engineering applications. *Carbohydrate Polymers*, 77, 863–869.
- Spasova, M., Manolova, N., Paneva, D., & Rashkov, I. (2006). Perspectives on: Criteria for complex evaluation of the morphology and alignment of electrospun polymer nanofibers. *Journal of Bioactive and Compatible Polymers*, 21, 465–479.
- Sun, K., & Li, Z. H. (2011). Preparations, properties and applications of chitosan based nanofibers fabricated by electrospinning. *E-XPRESS Polymer Letters*, 5, 342–361.
- Yang, D., Jin, Y., Zhou, Y., Ma, G., Chen, X., Lu, F., et al. (2008). In situ mineralization of hydroxyapatite on electrospun chitosan-based nanofibrous scaffolds. *Macromolecular Bioscience*, 8, 239–246.
- Zhang, Y., Venugopal, J. R., Turki, A. E., Ramakrishna, S., Su, B., & Lim, C. T. (2008). Electrospun biomimetic nanocomposite nanofibers of hydroxyapatite/chitosan for bone tissue engineering. *Biomaterials*, 29, 4314–4322.
- Zhang, J. F., Yang, D. Z., Xu, F., Zhang, Z. P., Yin, R. X., & Nie, J. (2009). Electrospun core-shell structure nanofibers from homogeneous solution of poly(ethylene oxide)/chitosan. *Macromolecules*, 42, 5278–5284.
- Zhang, C., Yuan, X., Wu, L., Han, Y., & Sheng, J. (2005). Study on morphology of electrospun poly(vinyl alcohol) mats. *European Polymer Journal*, 41, 423–432.
- Zhou, Y., Yang, D., Chen, X., Xu, Q., Lu, F., & Nie, J. (2008). Electrospun water-soluble carboxyethyl chitosan/poly(vinyl alcohol) nanofibrous membrane as potential wound dressing for skin regeneration. *Biomacromolecules*, 9, 349–354.